



Biosynthesis of PbO nanoparticles via *Adhatoda vesica* (*Justicia adhatoda*) leaves extract for antimicrobial and photocatalytic applications

S. Logambal^{a,*}, M. Chandrasekar^b, R. Ashok Kumar^c, C. Inmozhi^d, S. Aravindan^g,
R. Uthrakumar^{a,*}, Suresh Naveenkumar^e, Azhaguchamy Muthukumaran^e, K. Kaviyarasu^f

^a Department of Physics, Government Arts College (Autonomous), Salem 636007, Tamil Nadu, India

^b Department of Physics, TAG. Govt. Arts College, Tindivanam 604307 Tamil Nadu, India

^c Department of Physics, Thiruvalluvar Government Arts College, Rasipuram, Tamil Nadu 637401, India

^d Department of Physics, Government Arts College for Women, Salem 636008, Tamil Nadu, India

^e Department of Biotechnology, Kalasalingam Academy of Research and Education, Krishnankoil, Tamil Nadu, India

^f UNESCO-UNISA Africa Chair in Nanosciences/Nanotechnology Laboratories, College of Graduate Studies, University of South Africa (UNISA), Muckleneuk Ridge, PO Box 392, Pretoria, South Africa

^g Department of Physics, Chikkanna Government Arts College, Tirupur - 641602, Tamil Nadu, India

ARTICLE INFO

Keywords:

PbO nanostructures

Photoluminescence

Green Chemistry

Biology and the environment

Antibacterial properties

Environmental pollution

ABSTRACT

Research applications in biology and the environment can benefit greatly from nanoscience and nanotechnology. Aqueous leaf extract of *Adhatoda vesica* (AV) mediated the formation of lead oxide (PbO) nanoparticles in this study. A XRD analysis confirmed that the lead oxide nanoparticles (PbO NPs) synthesized from leaves extract have a crystalline structure. UV-vis spectroscopy study of colloidal PbO nanoparticles absorption revealed the greatest absorption bands, and the photoluminescence (PL) emission spectrum revealed a broad nature of visible emission peaks with high surface defects. By analyzing PbO nanoparticles using the fourier transform infrared method (FTIR), the leaf extract demonstrated the presence of functional peaks. It was evident from the SEM images that most of the PbO NPs had a spherical, irregular sponge-like shape. Additionally, the PbO nanostructures were tested for their antibacterial activity against *Escherichia Coli*, and a high level of antibacterial activity was observed, indicating their suitability for antimicrobial applications. PbO NPs have been evaluated for photocatalytic degradation of methylene blue dye (MB) under UV irradiation and have produced indications that the synthesized material is suitable for photocatalytic degradation. The *Adhatoda vesica* is used as medicine and enhances lead oxide nanomaterials' antibacterial properties. The research is focused on focusing on environmental pollution control and treatment of different diseases such as asthma, bronchitis, tuberculosis, and other diseases through applications of Ayurveda, Siddha, Homeopathy, and Unani. A study based on these findings revealed that *Adhatoda vesica* (*Justicia adhatoda*) leaves extract can be utilized as a cost-effective and environmentally friendly alternative to producing lead oxide nanoparticles.

1. Introduction

Nanotechnology is a rapidly evolving subject that has applications in the medicinal, chemical, biological, mechanical, electronic, and environmental industries (Chandrasekar et al., 2022; Perumal et al., 2023; Renuka et al., 2020; Sowmya Sri Rathnakumar, 2019; Chandrasekar et al., 2021). Metal oxide nanoparticles are typically regarded as having antibacterial properties among inorganic nanoparticles (Logambal et al., 2022; Manimegalai et al., 2014). The release of ions into the solution is thought to produce reactive oxygen species, which are harmful to

bacteria. According to other research, nanoparticles can penetrate bacterial cell walls and target organelles, resulting in cell death (Khan et al., 2012). Inorganic antibiotics, unlike organic antibiotics, offer multiple targeted routes to attack drug-resistant bacteria via mutations (Kaviyarasu et al., 2012; Thanigai Arul et al., 2017). Metal oxides offer simple synthesis pathways that can be managed to modify the size and shape of nanoparticles and have depletion owing to environmental pollution (or) hazardous reductions in nanoparticles. Many nanoparticles, such as silver and gold nanoparticles, have recently been manufactured using a variety of biological sources, including bacteria,

* Corresponding authors.

E-mail addresses: logambalpoojasri@gmail.com (S. Logambal), uthraloyola@yahoo.com (R. Uthrakumar).

<https://doi.org/10.1016/j.jksus.2024.103169>

Received 24 June 2022; Received in revised form 15 December 2023; Accepted 16 March 2024

Available online 20 March 2024

1018-3647/© 2024 The Author(s). Published by Elsevier B.V. on behalf of King Saud University. This is an open access article under the CC BY-NC-ND license (<http://creativecommons.org/licenses/by-nc-nd/4.0/>).

fungi, algae, and plants. It's worth noting that, unlike other metal oxides, PbO is an *n*-type semiconductor with a forbidden energy gap of 2.66 eV, is environmentally friendly, and can be utilized to make multifunctional air filtration membranes. Lead is found in both amorphous and crystalline forms and has a wide range of uses, including solar cells, drug delivery, photocatalysis, air filtration, and antibacterial applications (Kaviyarasu et al., 2012; Perumal et al., 2022; Raja et al., 2020; Fang et al., 2014). Efficient biological methods used in the production of PbO nanostructures are for various instances, leaf, flower bud, stem, root, and flower extracts. It has been essentially suggested that plant-based materials are promising candidates, and the process of synthesizing lead oxide nanostructures is very simple to scale up (Raja et al., 2019; Elayaraja et al., 2012; Panimalar et al., 2022; Kasinathan et al., 2016).

Adhatoda vesica (*Justicia adhatoda*) is a common medicinal plant that has been used for generations to cure a variety of ailments including asthma, tuberculosis, malaria fever, cough, and sprain. It has several photochemical components with unusual biological characteristics. This study summarizes the previous and current state of *Adhatoda vesica* research in terms of medicinal use, phytochemistry, pharmacological activities, toxicity profile, and therapeutic use to fill in the gaps that require further research. The plant contains diterpenes, flavonoids, xanthenes, noriridoides, and other unidentified chemicals. Antimicrobial, hepato-renal protecting, liver enzymes modulation insecticidal, and toxicological actions of plant extracts and pure substances have been described. In addition, the presence of a catalyst allows for lead oxide (PbO) for easy alteration of physical and chemical properties. It has been commonly used in various fields such as supercapacitors, optoelectronic devices, and catalytic applications due to the suitable bandgap energy (2.66 eV), which is advantageous for photocatalytic applications and photogenerated electron-hole (e^-/h^+) pairs from recombination. Because of their strong photocatalytic activity for the degradation of organic pollutants, the suppression of electron-hole pair recombination, and heavy absorption of $-OH$ ions on the catalyst surface all contributed to a rise in photocatalytic activity (Panimalar et al., 2020; Chandrasekar et al., 2022; Panimalar et al., 2022). The enhancement of photocatalytic activity may be attributed to electron trapping by oxide ions, smaller particle size, greater surface area, and more surface roughness. Generally, PbO nanoparticles with different doping have previously been proposed to rise the metal ion content, resulting in increased electrocatalytic activity. Furthermore, no paper on leaves extracts PbO nanoparticles has been evaluated to our knowledge. *Adhatoda vesica* colloidal PbO nanoparticles on methylene blue as photocatalysts for biological and environmental applications were studied for changes in the crystalline structure, surface morphology, and antibacterial and photocatalytic activity

2. Materials and method

2.1. Synthesis of leaves extracts PbO nanoparticles

The leaves of *adhatoda vesica* were washed thoroughly in tap water and rinsed briefly in deionized water to eliminate dust particles. In 250 ml, 10 g of washed and finely cut leaves were used to make the aqueous solution. The mixture was boiled at 60 °C for 15 min in an Erlenmeyer flask with 100 ml of deionized water, this extract was filtered and used in further studies. At 80 °C for 1 hr, 6 g/100 ml extracts of the precursor salt, lead acetate $[Pb(CH_3COO)_2]$, were homogeneously combined. Following that, the resultant solution showed mild acidification, with a final pH of ~ 4.6 . During the heating phase, precipitate development was detected. The resulting solution was allowed to settle to room temperature before the PbO precipitate was dried for one day at 100 °C in a drying oven. The dry powder was annealed for 2 hrs in an open-air furnace at 600 °C in a ceramic crucible, resulting in highly crystalline nanoparticles that changed color from green to brown.

2.2. Antibacterial activity

The antibacterial activity test was performed using a modified version of the Bauer method in 1966. The prepared Muller Hiltonn was autoclaved for 20 min at 15 lbs pressure and chilled to 45 °C. The cooling media was sprayed onto sterilized petri plates and allowed to set. Using a sterile swab, the plates with media are implanted with their respective microbial suspension. On each petri plate, the various solvent extract prepared discs were placed independently, as well as a control and standard (Nitrofurantoin 300 g) for the bacteria disc. The plates were incubated for one day at 37 °C, after which the generated zone diameter surrounding the paper disc was measured and revealed in millimeters.

3. Results and discussion

3.1. Analysis of X-ray diffraction

X-ray powder diffraction (XRD) analysis was used to determine the crystal lattice and structure of biosynthesized PbO nanoparticles. Fig. 1 (a) shows the X-ray diffraction spectrum of the bioinspired production of lead oxide nanoparticles. The crystallographic reflections of orthorhombic massicot and tetragonal litharge of lead oxide (PbO) with standard lattice parameters of $a = 0.549$ nm, $b = 0.589$ nm, and $c = 0.475$ nm were detected, which are similar with JCPDS pattern no. 00-038-1477 for massicot phase. The crystallographic planes of face-centered cubic (FCC) structures of lead nanoparticles (111), (200), (220), and (311) agree with the crystallographic planes of face-centered cubic (FCC) structures of lead nanoparticles (111), (200), (220), and (311), respectively. Therefore, the PbO structure is well represented by all the peaks. The nanocomposite's PbO diffraction peaks were broad, indicating a small crystallite size. Reflections of crystalline organic molecules maintained on the surface of PbO NPs account for the remaining minor peaks. The XRD pattern found was like previous publications on plant-based synthesis. The Debye-Scherrer equation is used to calculate the average crystallite size of nanoparticles.

$$D = 0.94\lambda / (\beta \cos\theta) \quad (1)$$

where, λ is the X-ray wavelength of CuK_{α} radiation = 1.5406 Å, [35], D is the FWHM of the diffraction peaks, β - FWHM in radian, θ - Bragg's angle. The Debye Scherrer equation is used to estimate the average crystallite size of PbO nanoparticles was 30.35 nm, and the most prominent peaks for the full width at half maximum (FWHM) from the XRD pattern was estimated using the as shown in Table 1.. There are two new pyrroloquinoline alkaloids, viz. A number of known compounds were isolated from the leaves of *Adhatoda vesica*, including 1,2,3,9-tetrahydropyrrolo (2,1-b)-quinazolin-9-one-3Rhydroxy-3(2'-dimethylamino phenyl) (desmethoxyaniflorine). The diffractogram did not show any impurity peaks, which proved that the lead nanoparticles were pure PbO.

3.2. UV-visible absorption spectral studies

The UV-visible spectra of synthesized lead oxide nanoparticles from the leaf extracts of *Adhatoda vesica* are shown in Fig. 1(b). Adequate production of PbO nanoparticles from the bio-reduction of lead oxide and lead ions is determined. This phenomenon was visually observed by the change in color of the solution mixture from pale blue to dark green after 30 mins. The color change of the solution can be explained by a bilateral electromagnetic field, which was induced by the concerted oscillation of free conduction electrons exhibiting the existence of *surface plasmon resonance* (SPR) (Manjula et al., 2018; Arularasu et al., 2018; Magdalane et al., 2021). The optical absorption on leaves extracts colloidal PbO nanoparticles depending on the particle size and medium and chemical surroundings. UV-vis spectroscopy analysis in the

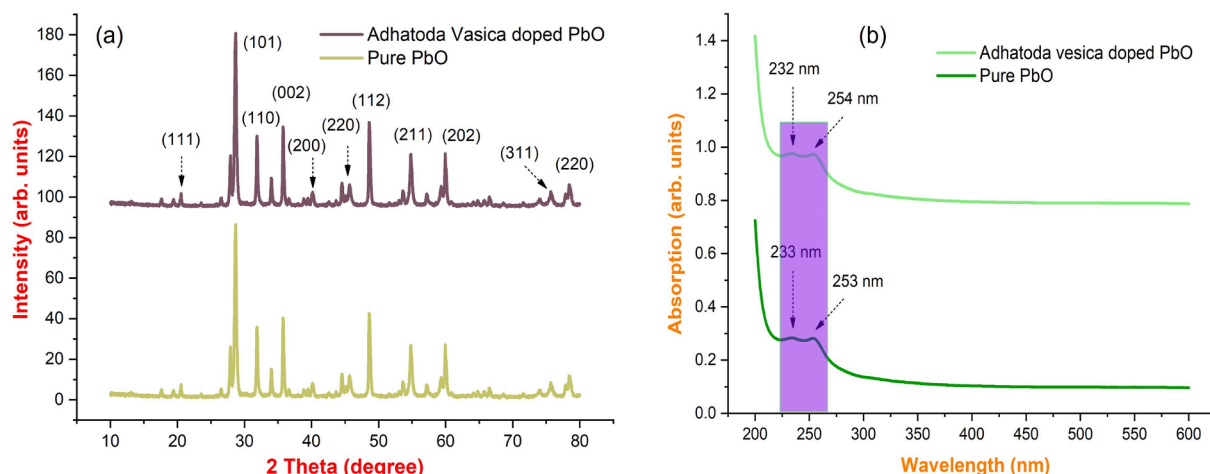


Fig. 1. (a-b). Fig. 1. X-ray diffraction pattern; (b) UV visible spectrum of synthesized PbO with *Adhatoda vesica* leaves extract nanoparticles.

Table 1

Particle size estimated from the X-ray diffraction spectrum of PbO nanoparticles.

S. No	Pos. [$^{\circ}$ 2Th.]	FWHM. [$^{\circ}$ 2Th.]	d-spacing [Å]	Particle size
1	38.0421	0.2460	2.36545	35.69
2	44.2284	0.2952	2.04789	30.35
3	64.4014	0.2460	1.44672	39.88
4	77.3702	0.3444	1.23342	30.88

wavelength range of 200 nm to 600 nm was used to track the development of the lead ion reduction. In these samples, nanoparticles are uniformly distributed, and most of them are nanoparticles as shown in 233 and 253 nm. Based on leaf extracts, the maximum absorption wavelength of lead oxide nanoparticles is 232 nm & 254 nm, indicating that the particles are mostly nanosized.

3.3. FTIR analysis

Phytochemicals often stabilize biosynthesized lead oxide nanoparticles through molecular interactions with metal surfaces. FTIR analysis can be used to analyze the nature of molecular interactions, and numerous capping agents have been proposed based on functional group reference peaks in the literature. In this study, we investigated the interaction between lead acetate and biomolecules present in *Adhatoda vesica* leaves extract. As shown in Fig. 2(a), we obtained several characteristic peaks 3369 cm^{-1} , 2362 cm^{-1} , 1609 cm^{-1} , 1118 cm^{-1} , 631 cm^{-1} , and 544 cm^{-1} , all of which were also obtained in bio-synthesized lead nanoparticles, implying that all these peaks correspond to molecules may be involved in the synthesis and stabilization of prepared nanoparticles. The amide groups from flavonoids, triterpenoids, and polyphenols are responsible for the peaks at 3369 cm^{-1} . As a result, the interaction between metal ions and amide groups in *Adhatoda vesica* leaf extract plays a role in the creation and stability (capping) of lead nanoparticles. Peaks at 2362 cm^{-1} could be attributed to phenolic -OH and -NH groups, amines, and the existence of alkane -CH stretching. The peak was observed at 1672 cm^{-1} stretching vibrations of C = O of -COOH. The peaks emerged at 1609 cm^{-1} due to carbon-carbon double bond. The sharp peak at 1118 cm^{-1} corresponds to C-N stretching vibrations aromatic amines.

3.4. Scanning electron microscope (SEM)

The size and shape of PbO nanoparticles produced with *Adhatoda vesica* leaves extract were visualized utilizing surface morphology. Fig. 2 (b, c) shows the SEM properties of the produced nanoparticles. Spherical, well-spread, and homogeneous particles were discovered. These

particles were made by reducing Pb ions to zero-valent atoms with coatings of various biological molecules with surface hydroxyl groups, resulting in agglomeration. The illustration of SEM showed somewhat sponge-like shaped nanoparticles produced with a diameter range of 250 nm to 500 nm. It indicates the completion of the nanoparticle synthesis process. The EDAX pictures of the pure and green synthesized PbO nanoparticles as shown in Fig. 2(d, e) the prepared sample clearly show the presence of major components such as Pb, Cu, and O, indicating that *Adhatoda vesica* leaf extract was successfully incorporated as C with PbO nanoparticles.

3.5. Antibacterial activities

Numerous analytical mechanisms have been followed to assess the antibacterial activity of PbO nanoparticles. According to the standard, the most susceptible process is the disc diffusion method. The antibacterial activity of leaves extract containing lead nanoparticles against *Staphylococcus aureus* and *Escherichia coli* were the results are depicted in Fig. 3(a, b) as the standard average values of zone inhibition. PbO nanoparticles show strong inhibitory activity against antibacterial species. The maximum zone inhibition of 28 mm was observed for *Staphylococcus aureus* the values are presented in Table 2 and PbO nanoparticles displayed higher bactericidal activity in *Staphylococcus aureus* when compared to Gram - negative bacteria *Escherichia coli*. However, no proper procedure of action of antibacterial lead was elucidated. Even though there are some viable approaches to determine whether a mixture of phospholipids connected to the bacterial membrane's proton pump disrupts the proton gradient. The antibacterial activity of comparable chemicals identified from the leaves of *Adhatoda vesica* has been attributed to a variety of mechanisms in the literature.

3.6. Antifungal activity

The results show that lead nanoparticles have good anti-fungal action against the *Aspergillus fumigata* microorganism. The ability of zinc nanoparticles to provide significant anti-fungal efficiency has been demonstrated, and thus PbO nanoparticles have a high potential activity, which is obvious in the inhibition zone by the growth of the tested microorganisms shown in Table 3. Fig. 3(c, d) depicts the activity of synthetic PbO nanoparticles derived from *Adhatoda vesica* plant extracts against *Aspergillus fumiga*. Using *Aspergillus fumiga*, anti-fungal activity in the diffusion assay, and evidence of fungi growth in the diffusion experiment, the anti-fungal properties of the PbO nanoparticles solution of leaf extract were examined (Geetha et al., 2018; Padmavathi et al., 2022; Logambal et al., 2023). The effect of synthetic PbO NPs derived from *Adhatoda vesica* plant extract against *Aspergillus fumiga*

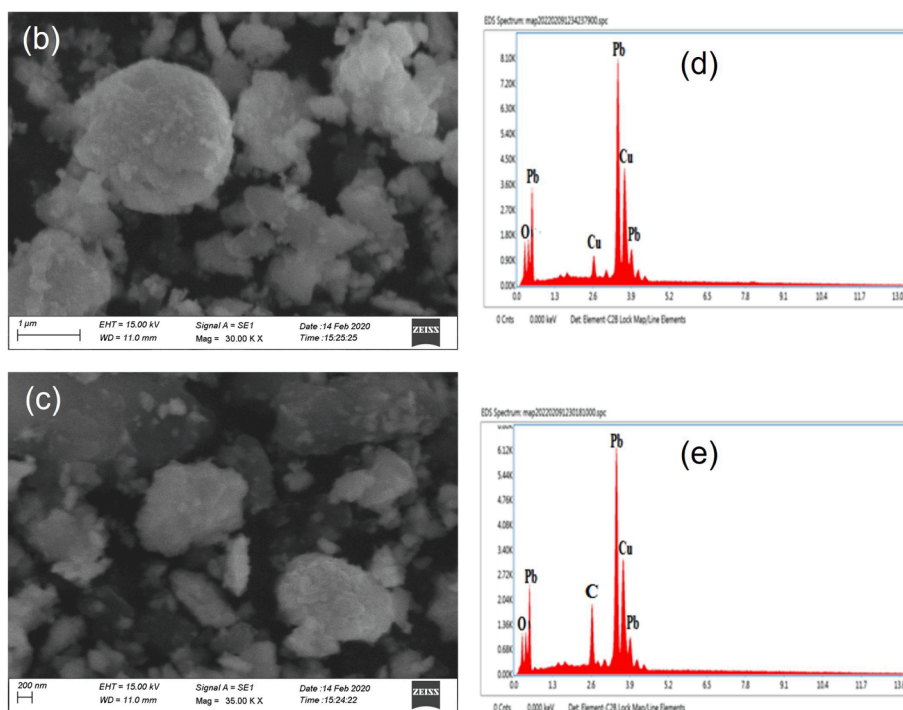
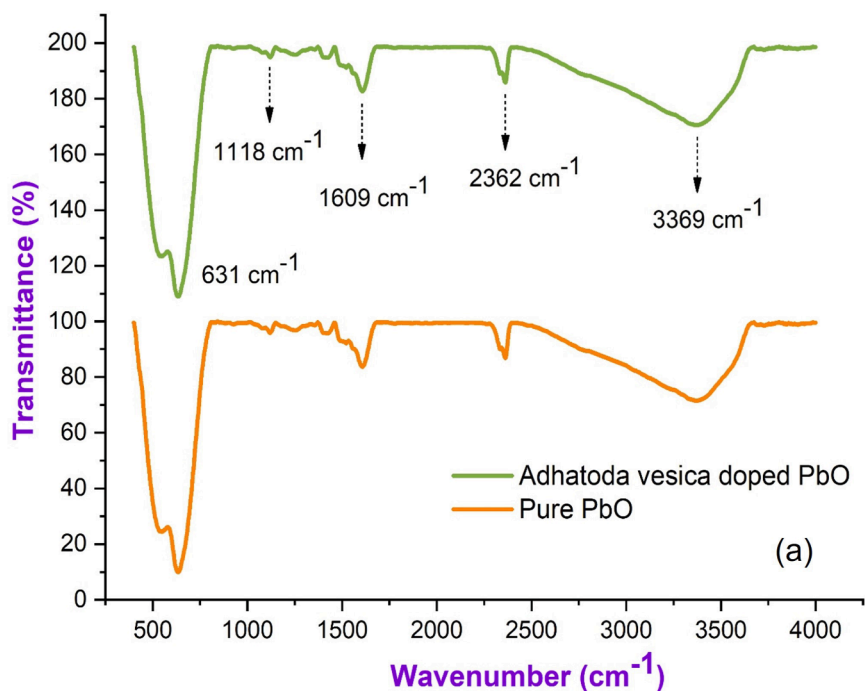


Fig. 2. (a) FTIR spectrum; (b-c) Scanning electron microscopy images; (d-e) EDAX spectrum of PbO with *Adhatoda vesica* leaves extract of synthesized PbO with *Adhatoda vesica* leaves extract.

has been determined. For 25 g/ml concentrations, the highest inhibition zone was 5 mm, while for 100 g/ml doses, it was 3 mm. As the concentration of *Aspergillus* fungus rises, the zone expands.

3.7. Photoluminescence spectral analysis

In the realm of photochemistry, the luminescence property of lead oxide nanoparticles is used. The structural features and accompanying defect levels are revealed by the precise emission wavelengths displayed in the spectrum. Fig. 4(a) shows the PL emission spectra of pure and

Adhatoda vesica leaf extract PbO nanoparticles. The presence of a blue emission peak of about 526 nm can be attributed to electron recombination (e^-/h^+) in the conduction band with deep doubly ionized oxygen vacancies, as shown in the picture. This can also be explained by excitonic recombination. There is no evidence of UV emissions towards the band edge, although this trait has been seen (George and D. Magimai Antoni Raj, X. Venci, A. Dhayal Raj, A. Albert Irudayaraj, S. John Sundaram, Amal A. Al-Mohameed, , 2022). Surface defects are represented by the green emission band at 403 nm, whereas the transition from the conduction band to singly ionized oxygen vacancies is shown by the

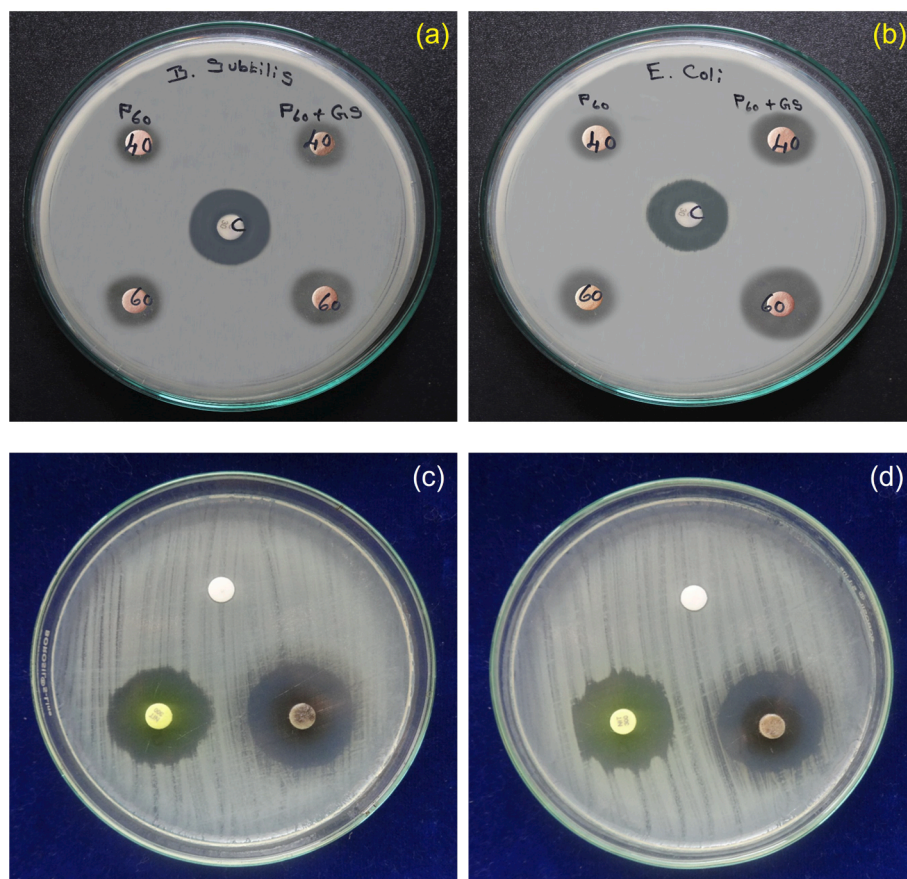


Fig. 3. (a-b) Antibacterial activity; (c-d) Antifungal activity of pure and PbO doped *Adhatoda vesica* leaves extract nanoparticles.

Table 2

Assay of antibacterial activity of *Adhatoda vesica* leaves extract PbO nanoparticles.

S. No.	Bacteria Name	Zone of Inhibition (mm in diameter)		
		Control	Standard*	S1
1	<i>Staphylococcus aureus</i>	–	25	29
2	<i>Escherichia coli</i>	–	24	28

Table 3

Antifungal activity of pure and *Adhatoda vesica* PbO nanoparticles.

S. No	Sample Marking	Sample Concentration (μl)	Zone of inhibition in (mm)
			<i>Aspergillus fumigata</i>
1	Control	PDA	NA
2	PbO AV	25	5
3		75	NA
4	Leaf Extract	50	NA
5		100	3

green emission band at 526 nm. Our research found no orange or red bands correlating to transitions associated to interstitial abnormalities. In addition, when comparing the two spectra, it is clear that the defect level intensities for PbO are substantially lower, reflecting a reduced defect density.

3.8. Photocatalytic activity

The degradation of heterocyclic organic dye MB under UV irradiation was investigated using PbO NPs with *Adhatoda vesica* extract as a

photocatalyst, which was hampered by phase composition, crystallite size, structure, bandgap, and other factors. The photocatalytic efficiency of *Adhatoda vesica* leaves extracting PbO as a function of time is shown in Fig. 4(b) the rate of absorbance perceived in terms of change in the MB max. The degrading impacts of both hues were used to validate the catalysts' capabilities. The transient degradation profile of methylene blue (MB) dye with all catalysts is illustrated in Fig. 4(c, d) under visible light. The degradation of heterocyclic organic dye MB under UV irradiation was investigated using PbO NPs with *Adhatoda vesica* extract as a photocatalyst, which was hampered by phase composition, crystallite size, structure, bandgap, and other factors (Vinayagam et al., 2023).

Using MB as a degradation aid, PbO nanoparticles with a degradation efficiency of 82 % was found in a sterile environment, which was good compared to other metal oxides nanoparticles (Perumal et al., 2022; Panimalar et al., 2022; Jayakumar et al., 2022). Fig. 5(a) depicts the method of photodegradation of MB by *Adhatoda vesica* leaves extract PbO. The photocatalyst absorbs the energy of a photon that is higher than its bandgap energy when exposed to UV light. The excitation of electrons from the valance band to the conduction band by a photon absorbed by *Adhatoda vesica* leaves extract PbO leads to charge separation, resulting in a negative electron in the conduction band and a positive hole in the valance band. The hole on the catalyst's surface combines with air moisture (OH•) and water (H₂O) to produce OH* and H⁺ radicals. The superoxide anion radical (O₂^{•-}) is formed when an electron liberated in the conduction band combines with molecular oxygen. The reaction pathway mechanism that occurred during the photocatalytic activity of the *Adhatoda vesica* leaves extract with PbO nanoparticles photocatalyst under visible light is shown in Fig. 5(b).

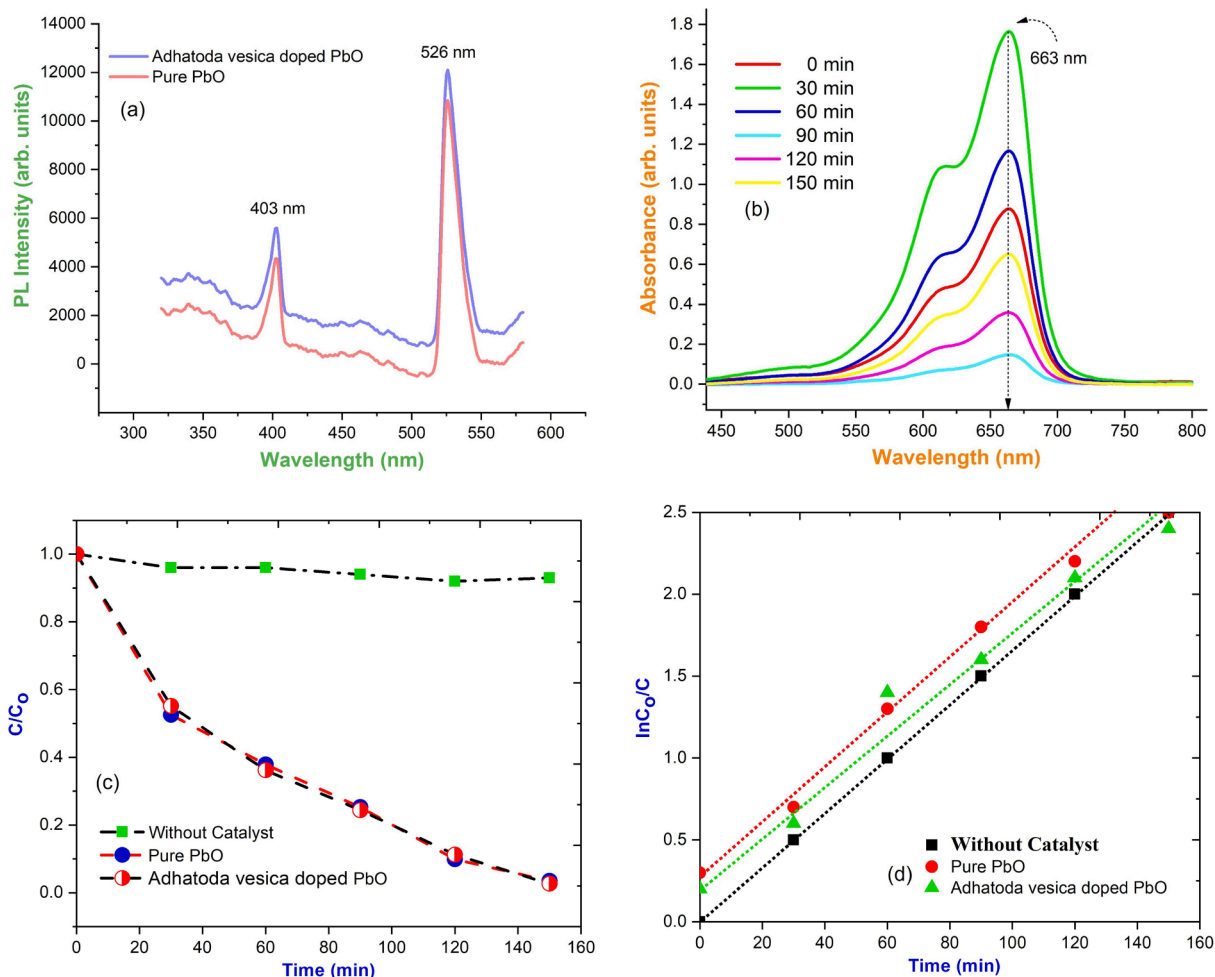


Fig. 4. (a) PL spectrum; (b) Photocatalytic activity spectrum of *Adhatoda vesica* leaves extract synthesized PbO nanoparticles; (c) Photocatalytic degradation efficiency of C/C_0 PbO nanoparticles; (d) Photocatalytic degradation efficiency of $\ln C_0/C$ vs time of PbO nanoparticles.

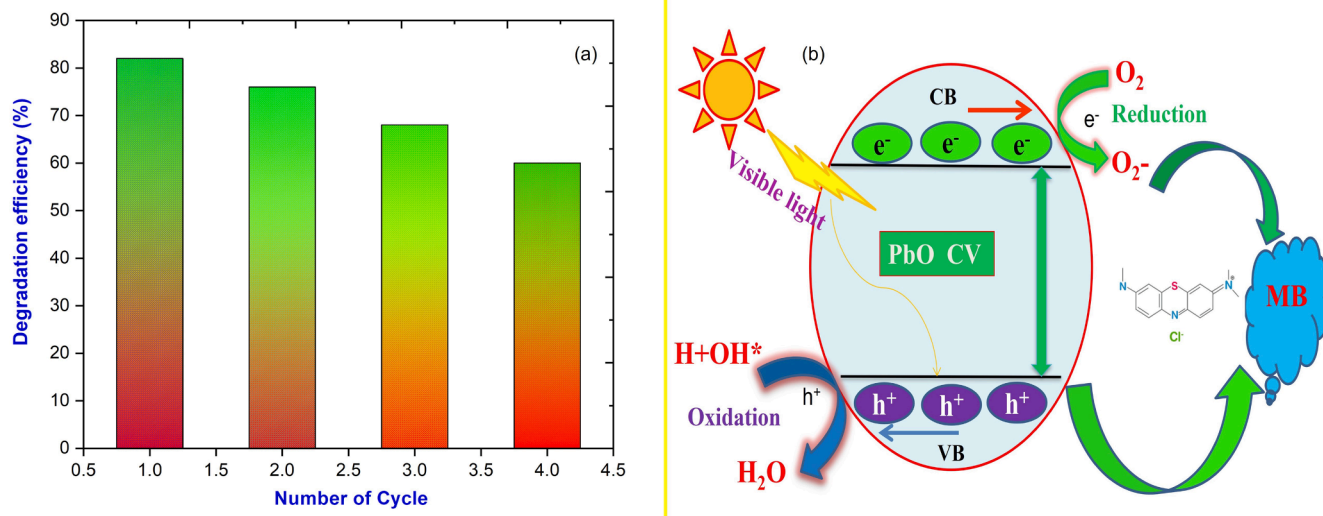


Fig. 5. (a) Photocatalytic degradation efficiency bar diagram; (b) Proposed photocatalytic reaction mechanism of *Adhatoda vesica* doped PbO photocatalyst.

4. Conclusion

The results of the present investigation achieve those leaves extracts of *Adhatoda vesica* are capable of fast, eco-friendly, economical, and

renewable synthesis of PbO nanoparticles. The XRD results revealed lead nanoparticles were well crystalline with face-centered cubic (FCC), trim dispersed sponge shape, and an average size ranging from 30 nm. The optical analysis confirmed the tuning of the optical bandgap in the range

2.12 eV – 2.66 eV concerning the mixed *Adhatoda vesica*. Impressively, leave extract colloidal PbO NPs exhibited a good dye degradation capability. SEM results showed the well-defined spherical-shaped PbO NPs and from the EDX confirmed the presence of elemental composition. The antimicrobial activity results showed that the *Adhatoda vesica* - PbO nanoparticles exhibited high inhibition against pathogenic bacteria. From the results, it is suggested that the *Adhatoda vesica* - PbO NPs can be used as effective growth inhibitors in various microorganisms. When compared to *Adhatoda vesica* leaf extract doped with PbO NPs exhibited degradation of methylene blue dye. The degradation efficiency is found to be 82 % was witnessed on enhanced photocatalytic activity of *Adhatoda vesica* PbO nanoparticles are suitable materials for environmental applications.

Funding interests

The authors declare that we have no relevant financial interests or conflicts related to this manuscript.

CRediT authorship contribution statement

S. Logambal: Investigation, Supervision, Project administration, Software, Writing – review & editing. **M. Chandrasekar:** Investigation, Formal analysis, Software, Writing – review & editing. **R. Ashok Kumar:** Methodology, Software, Visualization. **C. Immozhi:** Formal analysis, Methodology, Visualization. **S. Aravindan:** Validation. **R. Uthrakumar:** Supervision, Data curation, Project administration, Visualization, Validation, Writing – review & editing. **Suresh Naveenkumar:** Software, Formal analysis, Data curation. **Azhaguchamy Muthukumaran:** Validation, Formal analysis. **K. Kaviyarasu:** Visualization, Validation.

Declaration of competing interest

The authors declare that they have no known competing financial interests or personal relationships that could have appeared to influence the work reported in this paper.

Acknowledgement

The authors acknowledge Department of Physics, Periyar University, Salem - 636011, Tamil Nadu, India, for providing facilities to carry out the research work.

Declaration:

Competing interests.

The authors declare that they have no competing interests.

Author credit statement.

S. Logambal: Investigation, Supervision, Original draft, Project administration, Software, Writing - Review & Editing; M. Chandrasekar: Investigation, Formal analysis, Original draft, Software, Writing - Review & Editing; R. Ashok Kumar: Methodology, Software, Review, Editing & Visualization; C. Immozhi: Formal analysis, Methodology, Review & Visualization;

S. Aravindan: Validation, Writing & Editing; R. Uthrakumar: Supervision, Data curation; Project administration, Drafting, Visualization, Validation, Review, Writing & Editing; Suresh Naveenkumar: Software, Formal analysis & Data curation; Azhaguchamy Muthukumaran: Validation, formal analysis, Writing & Editing; K. Kaviyarasu: Visualization; Validation; Review & Editing;

References

Arularasu, M.V., Anbarasu, M., Poovaragan, S., Sundaram, R., Kanimozhi, K., Letsholathebe, D., Mola, G.T., 2018. Structural, optical, morphological, and microbial studies on SnO₂ nanoparticles prepared by co-precipitation method. *J. Nanosci. Nanotechnol.* 18 (5), 3511–3517.

- Chandrasekar, M., Panimalar, S., Uthrakumar, R., Kumar, M., Raja Saravanan, M.E., Gobi, G., Madheswaran, P., Immozhi, C., Kaviyarasu, K., 2021. Preparation and characterization studies of pure and Li⁺ doped ZnO nanoparticles for optoelectronic applications. *Mater. Today: Proc.* 36, 228–231.
- Chandrasekar, M., Subash, M., Logambal, S., Udhayakumar, G., Uthrakumar, R., Immozhi, C., Al-Onazi, W.A., Al-Mohaimed, A.M., Tse-Wei Chen, Kanimozhi, K., 2022. Synthesis and characterization studies of pure and ni-doped CuO nanoparticles by hydrothermal method. *J. King Saud Univ.- Sciences* 34, 101831.
- Chandrasekar, M., Subash, M., Perumal, V., Panimalar, S., Aravindan, S., Uthrakumar, R., Immozhi, C., Isaev, Abdugalam B., Sudhakar Muniyasamy, 2022. Specific Charge Separation of Sn Doped MgO Nanoparticles for Photocatalytic Activity under UV Light Irradiation. *Separation and Purification Technology* 294, 121189.
- Elayaraja, K., Rajesh, P., Ahymah Joshy, M.I., Sarath Chandra, V., Suganthi, R.V., Kennedy, J., Kulriya, P.K., Sulania, I., Asokan, K., Kanjilal, D., Avasthi, D.K., Varma, H.K., Narayana Kalkura, S., 2012. Enhancement of wettability and antibiotic loading/release of hydroxyapatite thin film modified by 100 MeV Ag⁷⁺ ion irradiation. *Mater. Chem. Phys.* 134, 464–477.
- Fang, F., Kennedy, J., Carder, D., Futter, J., Rubanov, S., 2014. Investigations of near infrared reflective behaviour of TiO₂ nanopowders synthesized by arc discharge. *Opt. Mater.* 36, 1260–1265.
- Geetha, N., Ayeshamariam, A., Siva Bharathy, M., Jayachandran, M., 2018. High performance photo-catalyst based on nanosized ZnO-TiO₂ nanoplatelets for removal of RhB under visible light irradiation. *J. Adv. Microsc. Res.* 13 (1), 12–19.
- George, A., Magimai Antoni Raj, D., Venci, X., Dhayal Raj, A., Albert Irudayaraj, A., John Sundaram, S., Al-Mohaimed, Amal A., 2022. Photocatalytic effect of CuO nanoparticles flower-like 3D nanostructures under visible light irradiation with the degradation of methylene blue (MB) dye for environmental application. *Environ. Res.* 203, 111880.
- Jayakumar, G., Irudayaraj, A.A., Raj, A.D., Sundaram, S.J., 2022. Electrical and magnetic properties of ni doped CeO₂ nanostructured for optoelectronic applications. *J. Phys. Chem. Solid* 160, 110369.
- Kasinathan, K., Kennedy, J., Elayaperumal, M., Henini, M., Malik, M., 2016. Photodegradation of organic pollutants RhB dye using UV simulated sunlight on ceria based TiO₂ nanomaterials for antibacterial applications. *Sci. Rep.* 6 (1), 1–12.
- Kaviyarasu, K., Sajan, D., Selvakumar, M.S., Augustin, S., Thomas, D.P., Anand, 2012. A facile hydrothermal route to synthesize novel PbI₂ nanorods. *J. Phys. Chem. Solid* 73, 1396–1400.
- Kaviyarasu, K., Devarajan, P.A., Xavier, S.S.J., Thomas, S.A., Selvakumar, S., 2012. One pot synthesis and characterization of cesium doped SnO₂ nanocrystals via a hydrothermal process. *J. Mater. Sci. Technol.* 28 (1), 15–20.
- Khan, Z., Ijaz Hussain, J., Adil Hashmi, A., 2012. Shape-directing role of cetyltrimethylammonium bromide in the green synthesis of ag-nanoparticles using neem (*Azadirachta indica*) leaf extract for colloids and surfaces B. *Biointerface* 95, 229–234.
- Logambal, S., Maheswari, C., Chandrasekar, S., Thilagavathi, T., Immozhi, C., Panimalar, S., Bassyouni, F.A., Uthrakumar, R., Ragab Abdel Gawwad, M., Aljowaie, Reem M., Al Farraj, Dunia A., Kanimozhi, K., 2022. Synthesis and characterizations of CuO nanoparticles using Couroupita guianensis extract for and antimicrobial applications. *J. King Saud Uni. Sci.* 34, 101910.
- Logambal, S., Immozhi, C., Ebanda Kedi, P.B., Bassyouni, F.A., Uthrakumar, R., 2023. Synthesis and antimicrobial activity of silver nanoparticles: incorporated couroupita guianensis flower petal extract for biomedical applications, *Journal of King Saud University – Science* 35, 102455.
- Magdalane, C.M., Priyadharsini, G.M.A., Simiyon, G.G., 2021. Synthesis and characterization of TiO₂ doped cobalt ferrite nanoparticles via microwave method: investigation of photocatalytic performance of Congo red degradation dye. *Surf. Interfaces* 25, 101296.
- Manimegalai, S., Sridharan, T.B., Rameshpathy, M., Rajeswari, D., 2014. Antioxidant, phytochemical screening and antimicrobial activity of couroupita guianensis flower extract. *Der Pharmacia Letter* 6 (6), 251–256.
- Manjula, N., Diallo, A., Ramalingam, G., Mohamed, S.B., Letsholathebe, D., Jayachandran, M., 2018. Structural, morphological and methanol sensing properties of jet nebulizer spray pyrolysis effect of TiO₂ doped SnO₂ thin film for removal of heavy metal ions. *J. Nanoelectron. Optoelectron.* 13 (10), 1543–1551.
- Padmavathi, J., Mani, M., Anantharaj, A., 2022. A study on the antibacterial activity of silver nanoparticles derived from *Corchorus aestuans* leaves and their characterization. *Chem. Phys. Lett.* 805, 139952.
- Panimalar, S., Uthrakumar, R., Tamil Selvi, E., Gomathy, P., Immozhi, C., 2020. Studies of MnO₂/g-C₃N₄ heterostructure efficient of visible light photocatalyst for pollutants degradation by sol-gel technique. *Surf. Interfaces* 20, 100512.
- Panimalar, S., Logambal, S., Thambidurai, R., Immozhi, C., Uthrakumar, R., Muthukumaran, A., Rasheed, R.A., Gatasheh, M.K., 2022. Effect of ag doped MnO₂ nanostructures suitable for wastewater treatment and other environmental pollutant applications. *Environ. Res.* 205, 112560.
- Panimalar, S., Subash, M., Uthrakumar, R., Immozhi, C., Al-Onazi, W.A., Al-Mohaimed, A.M., 2022. Reproducibility and long-term stability of sn doped MnO₂ nanostructures: Practical photocatalytic systems and wastewater treatment applications. *Chemosphere* 293, 133646.
- Panimalar, S., Subash, M., Chandrasekar, M., Uthrakumar, R., Immozhi, C., Al-Onazi, W. A., Al-Mohaimed, A.M., Tse-Wei Chen, J., Kennedy, 2022. Reproducibility and long-term stability of sn doped MnO₂ nanostructures: Practical photocatalytic systems and wastewater treatment applications. *Chemosphere* 293, 133646.
- Perumal, V., Sabarinathan, A., Chandrasekar, M., Immozhi, C., Uthrakumar, R., Raja, A., Elshikh, M.S., 2022. Hierarchical nanorods of graphene oxide decorated SnO₂ with

- high photocatalytic performance for energy conversion applications. *Fuel* 324, 124599.
- Perumal, V., Inmozhi, C., Uthrakumar, R., Robert, R., Chandrasekar, M., Beer Mohamed, S., Shehla Honey, A., Raja, F.h.A., Al-Mekhlafi, 2022. Enhancing the photocatalytic performance of surface - treated SnO₂ hierarchical nanorods against methylene blue dye under solar irradiation and biological degradation. *Environ. Res.* 209, 112821.
- Perumal, V., Uthrakumar, R., Chinnathambi, M., Inmozhi, C., Robert, R., Rajasaravanan, M.E., Raja, A., Kaviyarasu, K., 2023. Electron-hole recombination effect of SnO₂-CuO nanocomposite for improving methylene blue photocatalytic activity in wastewater treatment under visible light. *Journal of King Saud University - Science* 35, 102388.
- Raja, A., Selvakumar, K., Rajasekaran, P., Arunpandian, M., Asath Bahadur, S., Swaminathan, M., 2019. Visible active reduced graphene oxide loaded titania for photodecomposition of ciprofloxacin and its antibacterial activity. *Colloids Surf A Physicochem Eng Asp* 564 (5), 23–30.
- Raja, A., Rajasekaran, P., Selvakumar, K., Arunpandian, M., Asath Bahadur, S., Swaminathan, M., 2020. Visible active reduced graphene oxide-BiVO₄-ZnO ternary photocatalyst for efficient removal of ciprofloxacin. *Sep. Purif. Technol.* 233 (15), 115996.
- Renuka, R., Devi, R., Sivakami, M., Thilagavathi, T., Uthrakumar, R., Kaviyarasu, K., 2020. Biosynthesis of silver nanoparticles using *Phyllanthus Emblica* fruit extract for antimicrobial application, biocatalysis and agriculture. *Biotechnology* 24, 101567.
- Sowmya Sri Rathnakumar, 2019. Kana noluthando, arockia jayalatha kulandaiswamy, John bosco balaguru rayappan, Kaviyarasu kasinathan, John Kennedy, Malik maaza, stalling behaviour of chloride ions: a non-enzymatic electrochemical detection of α -endosulfan using CuO interface. *Sens. Actuators B* 293, 100–106.
- Thanigai Arul, K., Manikandan, E., Murmu, P.P., Kennedy, J., Henini, M., 2017. Enhanced magnetic properties of polymer-magnetic nanostructures synthesized by ultrasonication. *J. Alloy. Compd.* 720, 395–400.
- Vinayagam, R., Kandati, S., Murugesan, G., Concepta Goveas, L., Baliga, A., Pai, S., Selvaraj, R., 2023. Bioinspiration synthesis of hydroxyapatite nanoparticles using eggshells as a calcium source: evaluation of Congo red dye adsorption potential. *J. Mater. Res. Technol.* 22, 169–180.

Further Reading

- Ahmad, S.A., Javed, S., 2007. Exploring the economic value of underutilized plant species in ayubia National Park. *Pak. J. Bot.* 39, 1435–1442.